Int J Earth Sci (Geol Rundsch) (2014) 103:1929–1944
DOI 10.1007/s00531-013-0917-1

ORIGINAL PAPER

Insights from trace element geochemistry as to the roles of subduction zone geometry and subduction input on the chemistry of arc magmas

Heidi Wehrmann · Kaj Hoernle · Dieter Garbe-Schönberg · Guillaume Jacques · Julia Mahlke · Kai Schumann

Received: 14 July 2012 / Accepted: 20 May 2013 / Published online: 21 March 2014

Abstract Subduction zones of continental, transitional, and oceanic settings, relative to the nature of the overriding plate, are compared in terms of trace element compositions of mafic to intermediate arc rocks, in order to evaluate the relationship between subduction parameters and the presence of subduction fluids. The continental Chilean Southern Volcanic Zone (SVZ) and the transitional to oceanic Central American Volcanic Arc (CAVA) show increasing degrees of melting with increasing involvement of slab fluids, as is typical for hydrous flux melting beneath arc volcanoes. At the SVZ, the central segment with the thinnest continental crust/lithosphere erupted the highest-degree melts from the most depleted sources, similar to the oceanic-like Nicaraguan segment of the CAVA. The northern part of the SVZ, located on the thickest continental crust/lithosphere, exhibits features more similar to Costa Rica situated on the Caribbean Large Igneous Province, with lower degrees of melting from more enriched source materials. The composition of the slab fluids is characteristic for each arc system, with a particularly pronounced enrichment in Pb at the SVZ and in Ba at the CAVA. A direct compositional relationship between the arc rocks and the corresponding marine sediments that are subducted at the trenches clearly shows that the compositional signature of the lavas erupted in the different arcs carries an inherited signal from the subducted sediments.

Keywords Subduction zones · Trace element geochemistry · Hydrous flux melting · Marine sediment input · Chilean Southern Volcanic Zone · Central American Volcanic Arc

Electronic supplementary material The online version of this article (doi:10.1007/s00531-013-0917-1) contains supplementary material, which is available to authorized users.

H. Wehrmann (✉) · K. Hoernle · D. Garbe-Schönberg · G. Jacques · J. Mahlke · K. Schumann
SFB574, GEOMAR Helmholtz Centre for Ocean Research Kiel, Wischhofstr. 1-3, 24148 Kiel, Germany
e-mail: hwehrmann@geomar.de

K. Hoernle · J. Mahlke · K. Schumann
GEOMAR Helmholtz Centre for Ocean Research Kiel, Wischhofstr. 1-3, 24148 Kiel, Germany

D. Garbe-Schönberg
Institute of Geosciences, University of Kiel, Ludewig-Meyn-Str. 10, 24118 Kiel, Germany

Introduction

Fluids from the subducting slab play a fundamental role in driving arc volcanism. They promote mantle melting at depth and evoke explosive eruptions near the surface. The presence and behaviour of subduction fluids and related magma compositions are a function of a number of factors: they firstly depend on the composition of the subduction input materials, i.e. the variably hydrated subducting slab (igneous crust and serpentinised uppermost mantle), the overlying sediments, and possibly material eroded from the overriding plate in the forearc by subduction erosion (e.g. Kay and Kay 1993; Kay and Mpodozis 2002; von Huene and Scholl 1991; and references therein), or from the slab-metasomatised forearc mantle wedge through frictional stresses (Tatsumi 1986; Savov et al. 2007). The mantle wedge beneath the arc may show compositional differences, ranging from mid-ocean ridge basalt (MORB)- to enriched (E-)MORB-sourced mantle, possibly including ocean island basalt (OIB) components. Subduction parameters, e.g. slab ages, convergence rates, and geometric properties such as slab dip angles, thickness of the

mantle wedge and of the overriding plate, will affect the thermal conditions in the system, thus governing mineral dehydration reactions (e.g. Syracuse and Abers 2006; Hacker 2008; Syracuse et al. 2010; John et al. 2011; and references therein) and subsequently the extent of fluid transfer at depth. The addition of fluids to the asthenospheric wedge will in turn influence the degree of melting beneath the arc. During ascent, melts may assimilate material from the overriding plate, consisting of continental, transitional (e.g. accreted ophiolitic terranes and oceanic plateaux/large igneous provinces), oceanic lithosphere, or young to zero-age plutonic rocks and crystal mushes of immediately prior magmatism. The thickness of the overriding plate may affect magma migration rates, storage times, degree of magma differentiation, and amount of assimilation.

To understand better the relevance of any of the factors influencing the erupted melt compositions, we compare the following different subduction systems in this paper: the Chilean Southern Volcanic Zone (SVZ) and the Central American Volcanic Arc (CAVA). These arcs show salient differences in a number of parameters, such that the SVZ accommodates a continental end member with regard to crustal thickness of the upper plate (reaching >60 km beneath the northern part of the SVZ), while the CAVA is a transitional arc, extending from an oceanic plateau beneath Costa Rica through accreted mafic terranes in Nicaragua to El Salvador and then to thickening continental crust in Guatemala. Compositions of input materials (the igneous crust, i.e. MORB or a subducted hotspot track, and the marine sediments) and overall subduction geometries vary strongly between the arcs. Nevertheless, each arc system comprises segments with properties comparable to some segments in the other arc. By considering both the differing and the similar subduction parameters, the comparison of the arc output from the different subduction systems permits to filter the relative importance of the parameters influencing the compositions of the erupted arc rocks, thus allowing us to address the question of whether the nature of the overriding plate or the subduction input plays a more important role.

A variety of previous studies have characterised the major and trace element compositions of arc rocks of the SVZ (e.g. Hildreth and Moorbath 1988; Hickey et al. 1984; López-Escobar et al. 1992) and of the CAVA (e.g. Carr et al. 2007; Sadofsky et al. 2008; Hoernle et al. 2008; Gazel et al. 2009; Heydolph et al. 2012; and references therein). In this paper, we integrate geochemical data from Sadofsky et al. (2008), Hoernle et al. (2008), Heydolph et al. (2012), Wehrmann et al. (in review), and Jacques et al. (2013) with new data sets from the SVZ and from subducting marine sediments. The major goal of this study is to gain a better insight into the parameters controlling the geochemistry of subduction zone volcanic rocks through a comparison of different end-member type arc systems, concerning input, slab geometries, and the nature and thickness of the overriding plate (crust and mantle).

Geologic setting

The Chilean Southern Volcanic Zone

The SVZ (Fig. 1a) encompasses more than 60 large volcanic centres, in addition to numerous small cones and satellite vents between latitudes 33°S and 46°S, located along the western margin of South America. The volcanic activity results from the subduction of the Nazca Plate beneath the South American Plate with convergence rates ranging from 70 to 90 mm/year (Stern 2004). The dip of the subducting plate decreases northwards from 39° to 28° from latitude 42°S to 35°S, and then to less than 24° into a region of flat subduction north of 33°S, where volcanism ceases. The SVZ comprises a continental end member in arc systems with thicknesses of the overriding continental crust reaching up to 60 km in its northern part. Details of subduction geometry are provided in Fig. 2a.

Subduction input materials, consisting of MORB-type oceanic crust and overlying marine sediments, have been described as relatively homogeneous in composition along the SVZ (Hildreth and Moorbath 1988; Melnick and Echtler 2006). The age of the incoming plate subducting beneath the active arc ranges from ~15 Ma in the south at 43°S to ~32 Ma in the north at 33°N. Several fracture zones are situated on the Nazca Plate (the Mocha, Valdivia, Chiloé, and Guafo Fracture Zones; Fig. 1a). These fracture zones might be sites of increased input of water and altered oceanic crust into the subduction zone (Dzierma et al. 2012). In southern and central Chile, glaciation has had a major control on the sediment supply to the trench, and hence, climate variability may have modulated the balance between accretionary and erosional processes along the mid- and southern latitudes of the margin through time (e.g. Bangs and Cande 1997). At present, the forearc along the SVZ is accretionary.

We here subdivide the SVZ according to a segmentation given by Hildreth and Moorbath (1988) and Dungan et al. (2001), with a slight modification as also used by Wehrmann et al. (in review), into a Northern SVZ (NSVZ; 33–34.5°S), a Transitional SVZ (TSVZ; 34.5–38°S; the previously used southern boundary at 37°S is shifted to 38°S), a Central SVZ (CSVZ; 38–42.5°S), and a Southern SVZ (SSVZ, here represented by small volcanic centres at Volcán Michinmávida/Chaitén at 43°S). The boundaries are illustrated in Fig. 1a.

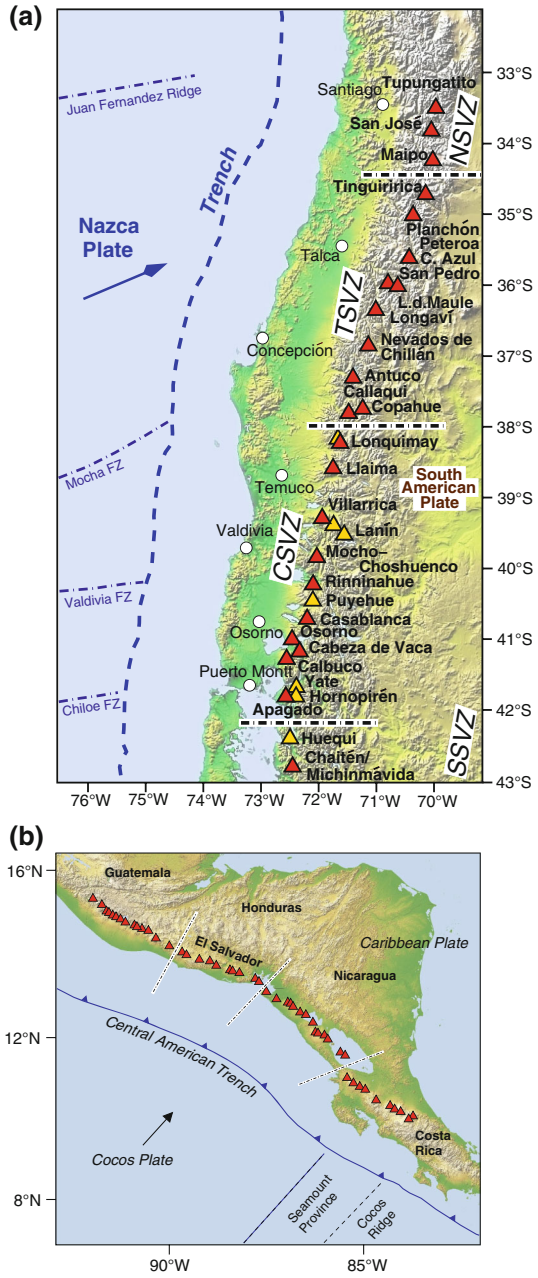

Fig. 1 Location map of **a** the Chilean Southern Volcanic Zone (SVZ) (*red triangles* depict studied volcanoes, *yellow triangles* indicate other young volcanic centres), **b** the Central American Volcanic Arc (CAVA) (*red triangles* indicate the volcanoes for which data have been evaluated in this study). Images of courtesy SRTM Team NASA/JPL/NIMA, modified

The Central American Volcanic Arc

The geologic setting of the CAVA (Fig. 1b) has been described in many previous studies (e.g. Carr 1984; Carr et al. 2007; Patino et al. 2000; Sadofsky et al. 2008; Wehrmann et al. 2011; and references therein). Volcanism at the CAVA extends over a distance of 1,100 km from north-western Guatemala to Central Costa Rica (CCR), produced by north-eastward subduction of the Cocos Plate beneath the Caribbean Plate at convergence rates of ~74–84 mm/year (DeMets 2001). It comprises dozens of major volcanic centres, including complex stratovolcanoes and caldera systems, in addition to numerous peripheral vents and small cinder cones. The overriding plate is of oceanic nature in the south-western arc segments. In Costa Rica, it consists of the Caribbean Large Igneous Province, in Nicaragua and part of El Salvador, and the crust is made up of oceanic plateaux and accreted mafic terranes. A transition to continental crust of the overriding plate occurs in El Salvador, becoming progressively thicker towards Guatemala. Subduction geometry, illustrating the differences in upper-plate thickness, melting column lengths, and angles of the downgoing slab, is shown in the along-arc profile in Fig. 2b.

Materials transported into the subduction zone vary greatly between the incoming plate outboard of Costa Rica and the incoming plate outboard of Nicaragua to Guatemala. Approximately 15–20 Ma old crust formed at the Cocos-Nazca Spreading Centre and the Galapagos Spreading Centre, which also contains parts of the zoned Galapagos Hotspot Tracks (Cocos Ridge and Seamount Province to the north-west of the ridge), subducts beneath Costa Rica and western Panama (Werner et al. 1999, 2003; Hoernle et al. 2000, 2002, 2008; Sadofsky et al. 2008). Offshore Nicaragua to Guatemala, subducting sediments on the incoming plate, as defined from Deep Sea Drilling Project (DSDP) Site 495, consist of a basal unit with ~250 m of carbonate ooze and a second overlying unit of ~200 m of organic carbon-rich hemipelagic clay (Aubouin and von Huene 1982). This input of carbonate-bearing lithologies is at a global maximum (Tera et al. 1986; Carr et al. 1990; Plank et al. 2002). The subducting slab outboard north-western Central America was formed ~20–25 Ma ago at the East Pacific Rise and has normal (N-)MORB-type composition, which was inferred from ocean crust samples from Site 1256 (Sadofsky et al. 2009), from a faulted seamount outboard of Nicaragua (Werner et al. 2003), and from Sites 499 and 500 off Guatemala (Geldmacher et al. 2008). It has been shown that the uppermost mantle of the incoming plate outboard of Nicaragua has been hydrated and converted to serpentinite at the outer rise due to extensive bend-faulting down to mantle depths (Ranero et al. 2003; Grevemeyer et al. 2007; Ivandic et al. 2007).

The greatest, or most focused, fluid release is believed to occur beneath Nicaragua, constrained by various geophysical means including seismic imaging (e.g. Peacock et al. 2005; Abers et al. 2006; Rychert et al. 2008; and references therein), by low $\delta^{18}O$ compositions of the erupted rocks (Eiler et al. 2005), and by studies of volatiles in olivine-hosted melt inclusions (e.g. Sadofsky et al. 2008; Wehrmann et al. 2011; and references therein).

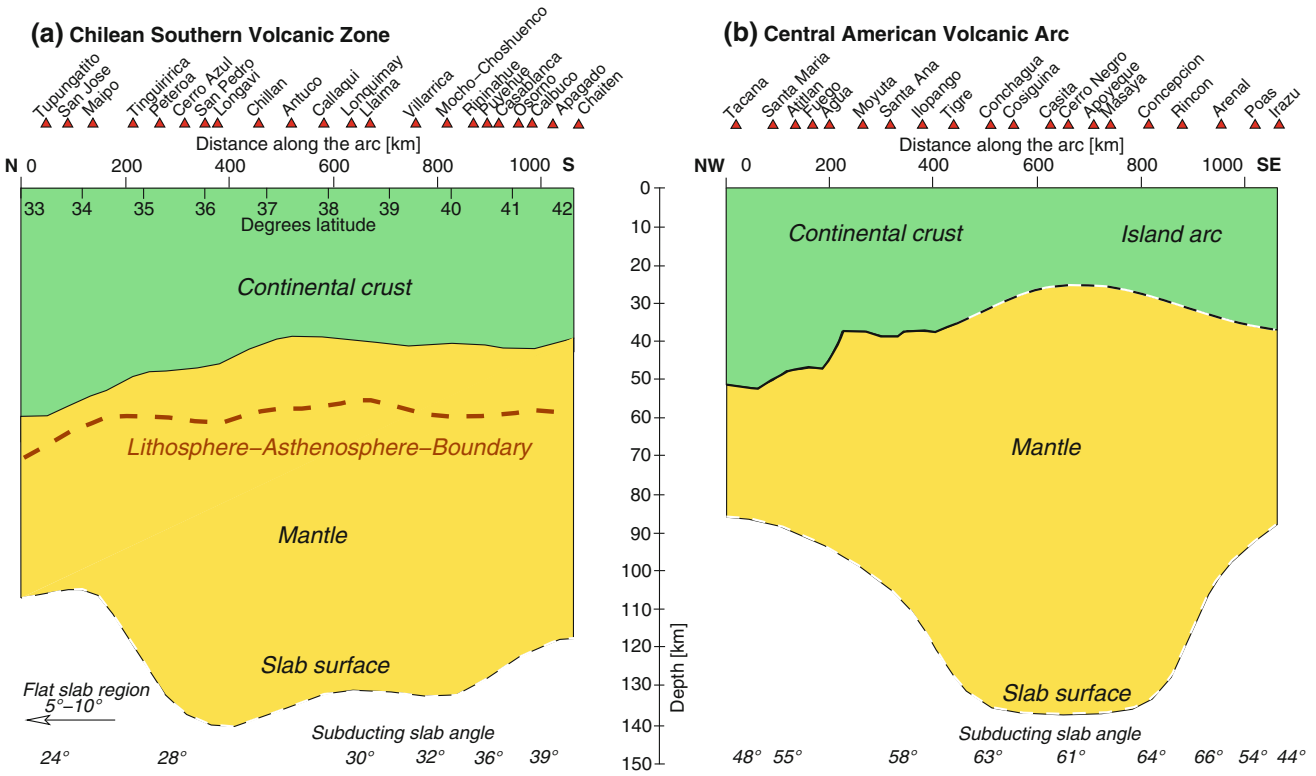

Fig. 2 Generalised along-arc profile of **a** the Chilean SVZ and **b** the CAVA, both extending ~1,100 km, illustrating variations in slab depth, crustal thickness, and melting column length. Arc volcanoes are also shown. SVZ geometry modified from Völker et al. (2011) based on models of Tassara et al. (2006). CAVA geometry modified from Wehrmann et al. (2011) using slab depths (generalised) and Guatemalan crustal thickness from Syracuse and Abers (2006), crustal thicknesses of Nicaragua and Costa Rica from MacKenzie et al. (2008)

Samples and data

For the large-scale geochemical coverage of the volcanic arcs, young mafic to intermediate tephra and lava samples were collected during a number of field campaigns along the volcanic fronts of Central America and southern Chile between 2002 and 2011. The major and trace element data presented here are compiled for the CAVA from Hoernle et al. (2008), Sadofsky et al. (2008), and Heydolph et al. (2012). For the SVZ, 96 new rock samples were analysed (Online Resource 1) and incorporated with 31 samples from Jacques et al. (2013), 20 samples from Wehrmann et al. (in review) (Online Resource 2), and one analysis from Volcán Huequi from Watt et al. (2011). All major and trace element data presented in the figures except for the one from Huequi were generated by the same procedures and the same instruments, giving analytical consistency and therefore comparability.

To characterise subduction input materials, several sea floor samples are included in this study. For the CAVA, geochemical data were obtained for sediments and altered ocean crust from ocean drilling project (ODP) Site 1256 (Sadofsky et al. 2009; Geldmacher et al. 2013), from DSDP Sites 495, 499, and 500 (Online Resource 1 and Table 1, this study, and Heydolph et al. 2012), and averaged sediment compositions were provided by Patino et al. (2000). Off the coast of the Chilean SVZ, a number of marine sediment samples were obtained from the sea floor during the RV Sonne Cruise 210. Sediment compositions on these samples were determined by Jacques et al. (2013). Our Chilean marine sediment data set is complemented by data from Lucassen et al. (2010).

Methods

The tephra and lava samples were hand-picked for fresh, juvenile material, and powdered. Sediment samples were powdered as bulk material. Whole-rock major element analyses of the volcanic samples were carried out with a Philips X'Unique PW 1480 XRF instrument at GEOMAR, Kiel, and the sediments were analysed on a MagixPro PW 2540 XRF at the University of Hamburg. For the trace element analyses, conventional table-top digests were made in PFA vials at 160 °C with HF-aqua regia-perchloric acid following the multi-step procedure established by Garbe-Schönberg (1993). Sediment samples were stored in high-pressure, high-temperature bombs for 4 days prior

Table 1 Marine sediment composition offshore the SVZ and the CAVA (μg/g)

	Sr	Nb	Cs	Ba	La	Ce	Yb	Pb	Th	U
Nacza Plate and continental slope sediments offshore Chile (Jacques et al. 2013)										
SO210-01-B (incoming plate)	258	5.14	8.07	1,681	15.4	33.4	2.22	20.5	6.16	3.97
SO210-01-T (incoming plate)	468	4.80	6.86	2,239	16.4	35.4	2.22	18.0	5.82	1.35
SO210-05-B (incoming plate)	257	4.63	5.54	1,238	13.5	32.4	1.97	17.5	5.70	3.21
SO210-05-T (incoming plate)	269	4.90	5.73	1,869	13.8	31.2	2.10	16.1	5.53	4.36
SO210-13-B (incoming plate)	319	4.48	4.97	1,137	14.3	33.4	2.11	18.0	5.30	4.54
SO210-13-T (incoming plate)	383	3.83	3.36	871	13.1	30.6	1.93	12.2	3.97	1.67
SO210-12-B (incoming plate)	273	4.40	4.91	1,190	12.8	30.1	1.95	14.2	5.02	3.80
SO210-12-T (incoming plate)	340	4.67	4.46	901	13.8	32.6	1.97	14.6	5.10	4.64
SO210-43-B (continental slope/Biobio slide)	484	3.33	2.28	294	11.9	27.4	1.79	9.40	3.50	1.15
S2O10-43-T (continental slope/Biobio slide)	360	4.34	3.41	317	14.2	32.8	2.07	11.3	4.61	2.39
Nacza Plate and continental slope sediments offshore Chile (Lucassen et al. 2010, subset)										
31SL(1)	335	8.30	4.56	512	16.6	36.5	2.13	26.0	5.61	2.22
115KD	358	6.80	3.51	343	14.9	33.2	2.22	12.8	4.47	1.36
32KD	312	7.40	2.09	327	14.2	31.1	2.21	9.49	4.39	2.86
33SL(1)	462	6.30	1.98	307	12.5	27.7	1.92	8.56	3.22	1.05
113SL(2)	287	4.58	3.79	653	12.9	28.7	1.83	11.7	4.55	2.85
112SL(1)	256	5.22	3.18	497	13.8	30.8	1.96	11.8	4.80	2.08
50SL(1)	335	8.80	3.58	454	17.7	38.5	2.28	15.8	5.52	1.80
100SL(1)	315	7.70	3.59	468	16.5	36.8	2.38	16.1	5.23	3.48
57KD	333	7.00	2.17	376	13.5	29.6	2.05	8.90	3.49	1.05
70KD	397	4.52	2.38	390	14.4	32.5	2.32	11.3	3.84	3.34
75KD(1)	272	5.00	1.33	294	13.5	29.7	1.91	7.99	4.22	1.06
90SL(1)	371	4.87	2.24	542	14.1	32.5	2.18	11.2	4.09	2.10
97KD	359	4.26	1.40	307	12.3	26.8	1.72	7.02	3.55	0.82
Cocos Plate sediments offshore CAVA (this study, and Heydolph et al. 2012)										
67_0495_031R_02W_51-53, carbonate sediment	1,366	0.27	0.11	2,148	8.22	1.99	1.12	4.67	0.13	0.19
67_0499B_004R_02W_80-82, carbonate sediment	1,325	0.18	0.11	1,972	6.78	1.31	0.87	3.56	0.09	0.24
67_0500_017R_03W_60-62, carbonate sediment	889	0.12	0.06	1,028	4.81	0.94	0.64	2.46	0.04	0.10
67_0500_014R_02W_85-87, carbonate sediment	1,096	0.15	0.07	1,911	5.37	1.02	0.68	2.45	0.07	0.36
67_0499_003R_02W_58-60, hemipelagic sediment	258	3.89	3.32	696	12.0	24.7	1.86	18.1	3.37	2.92
67_0495_019R_03W_73-75, hemipelagic sediment	308	3.64	2.70	240	11.9	23.3	2.05	6.57	2.32	4.57
67_0499_019R_05W_80-82, hemipelagic sediment	330	4.71	3.46	188	11.7	24.3	1.96	5.54	3.12	7.91
CAVA mean carbonate sediments (Patino et al. 2000)	1,504	0.44	0.15	2,145	8.78	2.40	1.18	3.70	0.16	0.15
CAVA mean hemipelagic sediments (Patino et al. 2000)	336	5.03	2.17	3,941	17.96	28.05	2.78	9.59	3.00	4.89

	Ba/La	Ba/Th	Ba/Nb	Sr/Th	Sr/Yb	Sr/Ce	U/Th	U/La	Pb/Ce	Pb/Yb
Nacza Plate and continental slope sediments offshore Chile (Jacques et al. 2013)										
SO210-01-B (incoming plate)	109	273	327	42	117	7.73	0.644	0.257	0.612	9.23
SO210-01-T (incoming plate)	136	384	466	80	210	13.2	0.232	0.082	0.507	8.08
SO210-05-B (incoming plate)	92	217	267	45	130	7.93	0.563	0.238	0.542	8.91
SO210-05-T (incoming plate)	136	338	381	49	128	8.60	0.788	0.317	0.516	7.67
SO210-13-B (incoming plate)	80	214	254	60	151	9.57	0.857	0.318	0.539	8.51
SO210-13-T (incoming plate)	67	220	227	97	198	12.5	0.421	0.128	0.399	6.33
SO210-12-B (incoming plate)	93	237	271	54	140	9.07	0.757	0.297	0.471	7.27
SO210-12-T (incoming plate)	65	177	193	67	173	10.4	0.91	0.336	0.449	7.43
SO210-43-B (continental slope/Biobio slide)	25	84	88	138	270	17.6	0.329	0.096	0.343	5.25
S2O10-43-T (continental slope/Biobio slide)	22	69	73	78	174	11.0	0.518	0.168	0.344	5.45

Table 1 continued

	Ba/La	Ba/Th	Ba/Nb	Sr/Th	Sr/Yb	Sr/Ce	U/Th	U/La	Pb/Ce	Pb/Yb
Nacza Plate and continental slope sediments offshore Chile (Lucassen et al. 2010, subset)										
31SL(1)	31	91	62	60	157	9.18	0.40	0.13	0.71	12.2
115KD	23	77	50	80	161	10.8	0.30	0.09	0.39	5.77
32KD	23	74	44	71	141	10.0	0.65	0.20	0.31	4.29
33SL(1)	25	95	49	143	241	16.7	0.33	0.08	0.31	4.46
113SL(2)	51	144	143	63	157	10.0	0.63	0.22	0.41	6.39
112SL(1)	36	104	95	53	131	8.31	0.43	0.15	0.38	6.02
50SL(1)	26	82	52	61	147	8.70	0.33	0.10	0.41	6.93
100SL(1)	28	89	61	60	132	8.56	0.67	0.21	0.44	6.76
57KD	28	108	54	95	162	11.3	0.30	0.08	0.30	4.34
70KD	27	102	86	103	171	12.2	0.87	0.23	0.35	4.87
75KD(1)	22	70	59	64	142	9.16	0.25	0.08	0.27	4.18
90SL(1)	38	133	111	91	170	11.4	0.51	0.15	0.34	5.14
97KD	25	86	72	101	209	13.4	0.23	0.07	0.26	4.08
Cocos Plate sediments offshore CAVA (this study, and Heydolph et al. 2012)										
67_0495_031R_02W_51-53, carbonate sediment	261	16,655	8,065	10,591	1,215	687	1.44	0.02	2.35	4.15
67_0499B_004R_02W_80-82, carbonate sediment	291	22,711	10,900	15,263	1,528	1,008	2.75	0.04	2.71	4.11
67_0500_017R_03W_60-62, carbonate sediment	214	23,669	8,533	20,464	1,395	947	2.28	0.02	2.62	3.86
67_0500_014R_02W_85-87, carbonate sediment	356	28,886	12,539	16,564	1,609	1,073	5.49	0.07	2.40	3.59
67_0499_003R_02W_58-60, hemipelagic sediment	58	207	179	77	139	10.5	0.87	0.24	0.73	9.74
67_0495_019R_03W_73-75, hemipelagic sediment	20	103	66	133	150	13.2	1.97	0.38	0.28	3.21
67_0499_019R_05W_80-82, hemipelagic sediment	16	60	40	106	168	13.6	2.53	0.68	0.23	2.82
CAVA mean carbonate sediments (Patino et al. 2000)	244	13,409	4,876	9,401	1,275	627	0.94	0.02	1.54	3.14
CAVA mean hemipelagic sediments (Patino et al. 2000)	219	1,314	784	112	121	12.0	1.63	0.27	0.34	3.45

to digestion to ensure complete digestion of zircons. Trace element compositions of the bulk rocks were determined with an Agilent 7500cs ICP-MS instrument at the Institute of Geosciences, University of Kiel in Germany. The results were confirmed to be analytically repeatable, reproducible, and true by several means: (1) every tenth sample was digested in duplicate; (2) the same digest solutions of several randomly chosen samples were repeatedly measured (3–5 times) within each analytical run to ensure consistency of the ICP-MS instrument, (3) a subset of approximately 100 digests was re-analysed in a single run with a dedicated washout protocol, and (4) external reproducibility/trueness was verified by means of a set of reference materials: BHVO-1, BHVO-2, AGV-1, JA-2, BIR-1, and JB-1a (Online Resource 3). Both laboratory blanks and instrumental background were monitored with different blank types included in each analytical run.

Results

On a K_2O versus SiO_2 classification diagram (Fig. 3, using subdivisions of LeMaitre et al. (1989) and nomenclature of Rickwood (1989)), the CSVZ rock array has the lowest K_2O. The TSVZ samples fall largely in the medium-K_2O, calc-alkaline field, similar to samples from Guatemala (GU), El Salvador (ES), and Nicaragua (Nic). Rocks from the NSVZ and the more evolved samples from Northern Costa Rica (NCR) reach into the high-K, calc-alkaline field, while the highest-K array is formed by samples from Central Costa Rica (CCR). Trace elements form typical subduction zone/island arc patterns in MORB-normalised multi-element diagrams (Fig. 4a–c), with pronounced troughs (relative depletion) at Nb and Ta, and peaks (relative enrichment) at highly fluid-mobile elements such as Ba, U, Pb, and Sr. Rocks from CCR show the least pronounced Nb and Ta negative and Pb-positive anomalies and overall show a more Galapagos-like ocean island basalt (OIB) signature, as was already described in previous studies (e.g. Reagan and Gill 1989; Benjamin et al. 2007; Sadofsky et al. 2008; Hoernle et al. 2008; Gazel et al. 2009). The incoming marine sediments (Fig. 4d) show enrichment of elements that become fluid-mobile during subduction. The carbonate sediments outboard the CAVA display the highest relative Ba and Sr, and lowest Rb, Pb, Th, and U contents. Averaged compositions of the SVZ

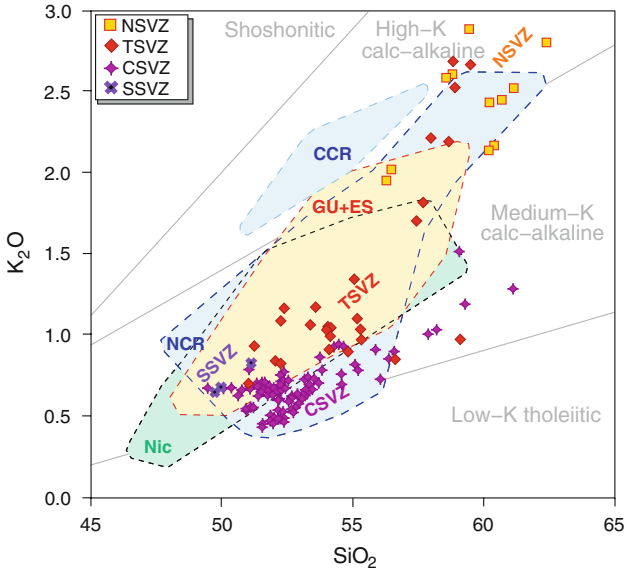

Fig. 3 K_2O versus SiO_2 of the SVZ (CSVZ *purple*, TSVZ *red*, and NSVZ *yellow–red diamonds*) in comparison to the CAVA (Guatemala (GU) and El Salvador (ES) *yellow*, Nicaragua (Nic) *green*, and northern (NCR) and Central Costa Rica (CCR) *light blue fields*)

and hemipelagic CAVA sediments have middle and heavy rare earth elements (REE) similar to MORB, while the carbonate sediments at the CAVA show strong relative depletion in REE. In terms of variations in trace element ratios along the arcs (Fig. 5a–h), both the SVZ and the CAVA involve segments with strongly elevated ratios of highly fluid-mobile to less fluid-mobile incompatible trace elements. There is an obvious geographic distinction in particular incompatible trace element ratios between the two arc systems. The Nicaraguan segment of the CAVA exhibits very high Ba/Th, Ba/Nb, U/Th, and Sr/Ce values, whereas the SVZ, in particular the CSVZ, displays strongly elevated Pb/Ce and Pb/U values. La/Yb and Nb/Y values peak in Costa Rica, while being low in the central to north-western CAVA. They are also low in the CSVZ, but show a gradual increase over the TSVZ towards the NSVZ.

Discussion

In the following, we use several trace elements as proxies for subduction processes and material involvement. Elements such as Ba, U, Pb, and Sr are termed "highly fluid-mobile", since they are readily scavenged by subduction fluids even at low temperatures (Kessel et al. 2005). "Less fluid-mobile" refers to Th and light REE, which are progressively released from the slab as the temperature increases, while middle and heavy REE are considered relatively fluid-immobile.

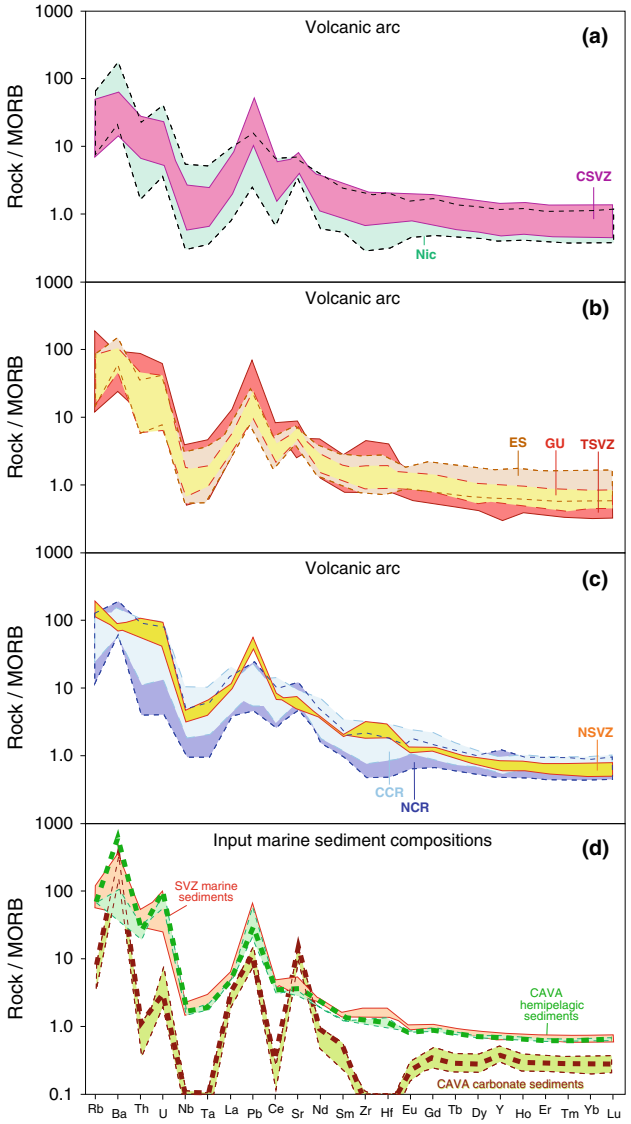

Fig. 4 N-MORB-normalised multi-element variation diagram [normalising values from Sun and McDonough (1989)] comparing **a** the CSVZ (*purple* field with *solid line*) with Nicaragua (*green* field with *dashed line*), **b** the TSVZ (*red* field with *solid line*) with Guatemala (*pale yellow* field with *long dashed line*) and El Salvador (*pale orange* field with *short dashed line*), **c** the NSVZ (*yellow* field with *solid line*) with Northern (*blue* field with *short dashed line*) and Central (*pale blue* field with *long dashed line*) Costa Rica, and **d** input marine sediment compositions also comparing the SVZ (red field with solid line) with the CAVA (carbonate sediments *brown-yellowish-green*, *dashed*; hemipelagic sediments *green*, *dashed*), whereby the *thick lines* reflect the bulk sediment compositions as estimated by Patino et al. (2000) for the CAVA

Compositional variation along the arcs

Strongly elevated values of canonical slab proxies in subduction systems, such as Ba/Th, Ba/Nb, U/Th, or Sr/Ce, occur within the Nicaraguan sample set, and decline towards both the north-western and south-eastern CAVA,

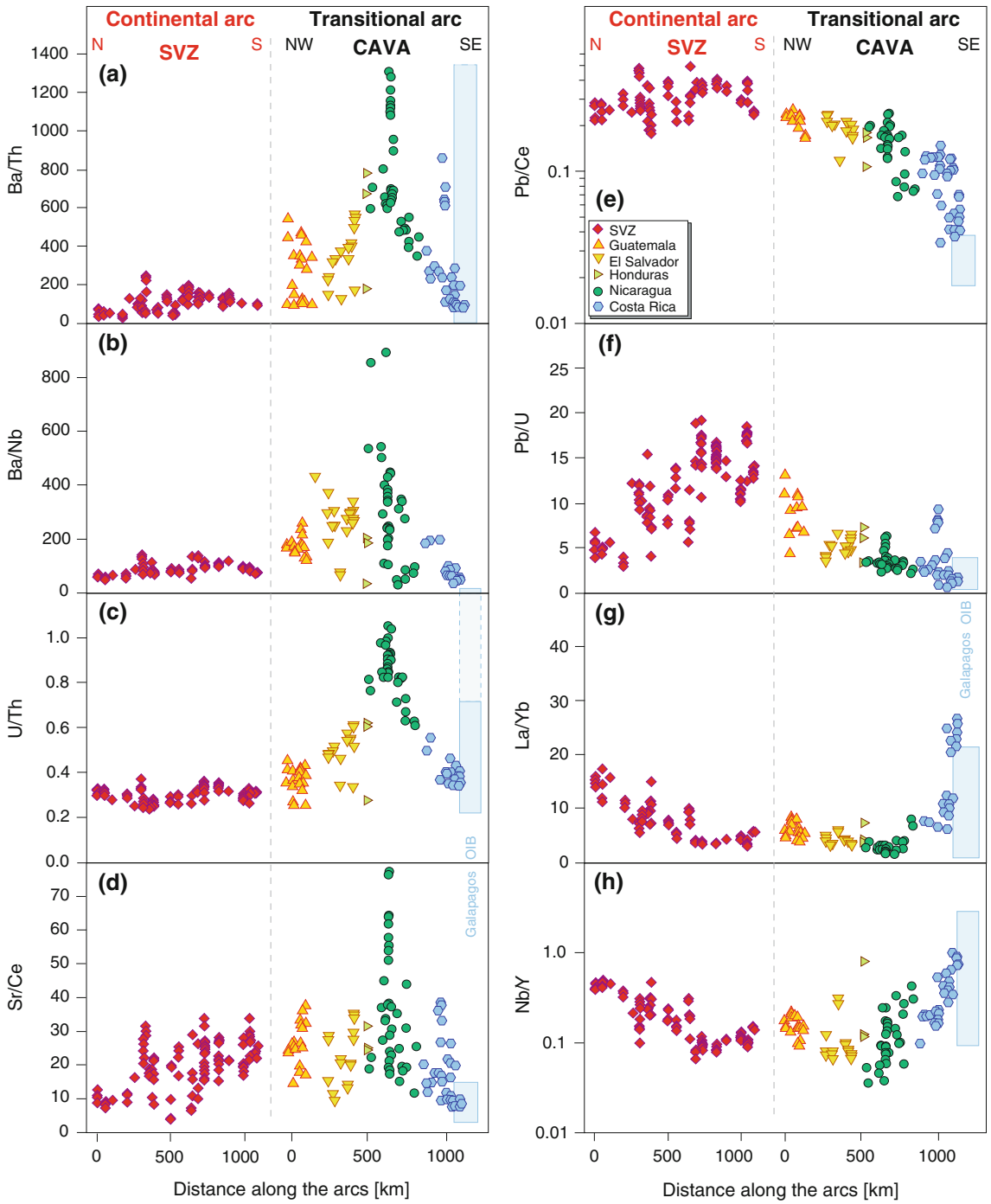

Fig. 5 Variation of trace element ratios along the Chilean SVZ (*left*, *red diamonds*) and the CAVA (*right*, *yellow*, *green*, and *blue symbols*). **a** Ba/La, **b** Ba/Nb, **c** U/Th, and **d** Sr/Ce ratios, despite their internal variability (Wehrmann et al., in review), are relatively uniform and low at the SVZ. At the CAVA, these ratios extend to higher values, reaching a maximum at Nicaragua. **e** Pb/Ce and **f** Pb/U reach the highest values at the SVZ, the latter in particular in the CSVZ. For **g** La/Yb and **h** Nb/Y, the highest values occur at the NSVZ of the SVZ and at the Costa Rican segment of the CAVA. The *shaded blue bars* indicate location and composition of the subducting seamount province of the Galapagos hot spot track [data from Hoernle et al. (2000)]

and are also considerably lower in the SVZ (Fig. 5a–d). Several previous studies also employed Ba/La, which displays a similar regional variation, but because of the differing partition coefficients of the two elements, the ratio can be affected both by slab and by mantle processes. The origin of this along-arc pattern of the CAVA is still subject of debate. It has been ascribed to the most channelised fluid flux from the steepest section of the slab beneath Nicaragua

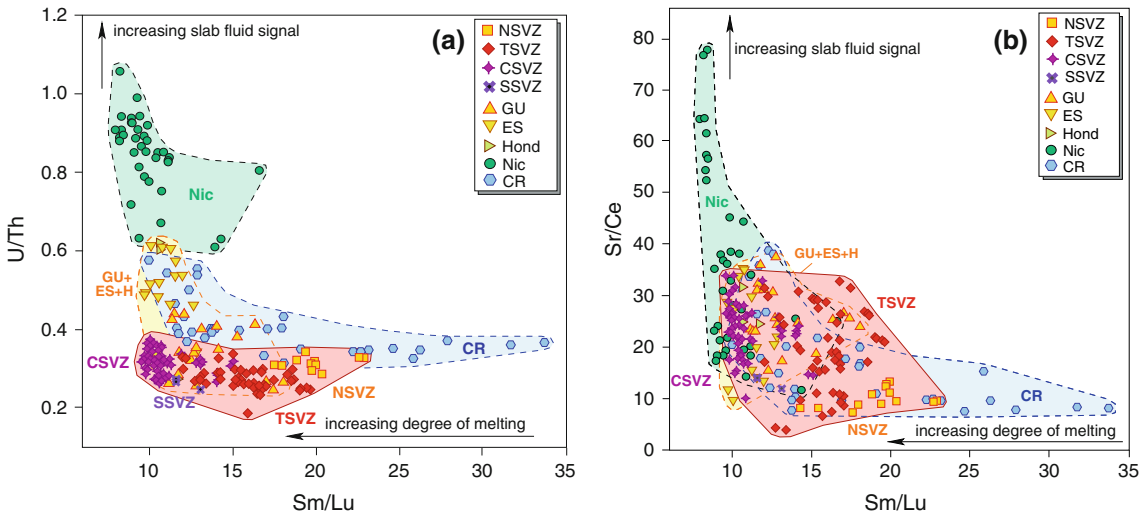

Fig. 6 **a** U/Th and **b** Sr/Ce versus Sm/Lu for the SVZ and the CAVA arc rocks, showing a typical pattern of hydrous flux melting with increasing U/Th and Sr/Ce at decreasing Sm/Lu, with exceptionally high values at the Nicaraguan segment of the CAVA. *Symbols* and *colours* as in Figs. 3 and 5

(Carr et al. 1990), or to highly variable fluid flow beneath different parts of the arc (e.g. Benjamin et al. 2007; Sadofsky et al. 2008). Other authors suggest variable involvement of sediments of different compositions (Plank and Langmuir 1993; Patino et al. 2000; Jicha et al. 2010). For the Ba/La ratio, it has also been proposed that the primary control is variation in La (Carr et al. 2007), which may reflect variations in the degree of melting of the mantle wedge (Sadofsky et al. 2008) and/or contribution from the melting of volcanic rocks in/on the downgoing slab (e.g. Hoernle et al. 2008; Gazel et al. 2009). At the SVZ, in contrast, these trace element ratios are comparatively uniform and low (in spite of their internal variability described by Wehrmann et al. in review) (Fig. 5a–d). Nb/U ratios are uniformly low in all CAVA and SVZ segments (<10; not shown) compared to the value of 47 ± 10 for oceanic basalts (MORB and OIB) from Hofman et al. (1986), reflecting enrichment of U relative to Nb by hydrous subduction fluids and melts.

A different pattern is observed for Pb/Ce and Pb/U ratios, which are highest at the southern-central SVZ, slightly lower in Guatemala, and gradually decreasing to El Salvador, Honduras, Nicaragua, and Costa Rica (Fig. 5e, f). The low values at Costa Rica and Nicaragua are considered to primarily reflect addition of melts from the subducting Galapagos hot spot track to the mantle wedge beneath CCR, and subsequent flow of this material northward as far as north-west Nicaragua (Hoernle et al. 2008; Gazel et al. 2009).

Assimilation of continental plutonic basement can also affect the highly fluid-mobile to less fluid-mobile element ratios, when long-term subduction recycling has concentrated highly fluid-mobile elements in the crust of the overriding plate by intrusion of highly fluid-mobile element-rich melts. In particular at the SVZ, many authors indeed favour a scenario of increasing interaction of the melts with progressively thickening crust towards the north (e.g. Hildreth and Moorbath 1988; Davidson et al. 1987; Ferguson et al. 1992). Based on U-series disequilibria, Reubi et al. (2011) concluded that assimilation of plutonic rocks in the volcano basement can be significant. Oxygen and Pb isotopes, however, show that crustal contamination is not the major factor controlling along-arc changes in the geochemistry of the SVZ arc lavas unless ancient Proterozoic lower crust is present beneath the NSVZ (Jacques et al. 2013 and G. Jacques, unpublished data).

These ratios of highly fluid-mobile to less fluid-mobile or fluid-immobile trace elements (Ba/Th, Ba/Nb, U/Th, Sr/Ce, Pb/Ce, and Pb/U) are commonly believed to serve as proxies for the delivery of fluids from the subducting slab to the mantle wedge. With regard to the issues raised above, the observed strong variation in these trace element ratios cannot directly be translated into different absolute amounts of fluids in the individual arc segments in a straightforward manner. Rather than simply representing varying amounts of fluids, the observed trace element patterns more likely point to differences in the fluid/melt compositions, in response to different subduction input materials and slab processes.

Lavas from CCR and the NSVZ have the highest La/Yb and Nb/Y ratios, which can be related to differing degrees of melting and/or an enriched mantle wedge component (Figs. 5g). In Costa Rica, this has been attributed to the addition of low-degree melts from the Galapagos hotspot track with high La/Sm, La/Yb, and Nb/Y to the mantle wedge (Hoernle et al. 2008; Gazel et al. 2009). The NSVZ

also shows high La/Yb, La/Sm, and Nb/Y but low Ba/Nb, U/Th, Sr/Ce, and Pb/U, which might, similar to the situation in Costa Rica, indicate that an enriched source component was involved in magma genesis beneath the NSVZ.

Hydrous flux melting

Typically, hydrous flux melting in subduction zones is associated with two characteristics: (a) high values of highly fluid-mobile to less fluid-mobile elements (e.g. U/Th, Sr/Ce, Ba/Th, Ba/Nb, and U/La), serving as proxies for high fluid flux, and (b) low ratios of more incompatible to less incompatible elements of relatively low fluid-mobility (e.g. La/Yb, Sm/Lu, Nb/Y, and Nb/Zr), reflecting high degrees of melting (e.g. Carr et al. 1990). We here use Sm/Lu as an indicator for the degree of melting instead of the widely employed La/Yb, because the latter suffers ambiguity arising from the mobilisation of La by subduction fluids at high temperatures and by possible addition from enriched source materials as described above. Sr/Ce, besides acting as an indicator for subduction fluids, is also affected by fractionation of plagioclase during magma evolution such that Sr is incorporated into the plagioclase, and the Sr/Ce ratio decreases when plagioclase precipitates from the melt. In the presence of fluids, however, the fractionation of plagioclase is suppressed (e.g. Grove and Baker 1984; Sisson and Grove 1993). Therefore, high Sr/Ce values likely reflect high fluid contents interrelated with limited plagioclase fractionation, while low Sr/Ce points to less fluids and accordingly Sr removal by plagioclase.

Serpentinite, if present in the crust and uppermost mantle for the incoming plate, is predicted to be a major source of fluids released from the slab beneath the arc (e.g. Ulmer and Trommsdorff 1999). Additionally, water may be contributed by dehydration of other mineral phases such as talc or chlorite (Spandler et al. 2008). Water release through deserpentinisation of the slab during subduction is a pressure–temperature-dependent reaction, whereby the temperature conditions play a key role (e.g. Hacker 2008; van Keken et al. 2011; Cooper et al. 2012). The slab temperature is generally a function of slab age, decreasing with increasing age of the slab, and it gradually increases as the slab proceeds to greater depths.

The inverse arrays formed between Sm/Lu with both U/Th and Sr/Ce (Fig. 6a, b) are consistent with high fluid fluxes into the mantle wedge, particularly beneath the CSVZ, Nicaragua, and El Salvador, resulting in the largest degrees of melting. Each of these areas is associated with the slab surface being more than 120 km beneath the mantle wedge, where the pressure–temperature conditions allow serpentine to break down and dehydrate. At the CAVA, there is clear evidence that serpentinite forms in the uppermost mantle of the incoming plate through bend-faulting at the outer rise of the subduction zone (Ranero et al. 2003; Grevemeyer et al. 2007; Ivandic et al. 2007). It is likely to play a key role also in the water transfer of the CSVZ via the incoming fracture zones. Subducting fracture zones are predicted to require lower temperatures to dehydrate at subarc depths (Hacker 2008). Moreover, although no detailed thermal modelling has to date been performed along the SVZ, the northward age progression of the incoming plate expectably produces higher temperatures beneath the CSVZ than beneath the TSVZ and the NSVZ, promoting a larger fluid contribution to the mantle wedge beneath the CSVZ. This peak fluid flow coincides with a peak in magma extrusion rate in the CSVZ in an along-SVZ consideration (Völker et al. 2011). This latter correlation does, however, not apply to all arc segments considered here. In Nicaragua, magma extrusion rates are low despite the high degrees of melting (Sadofsky et al. 2008). It has been proposed, however, that Nicaragua experiences large magma intrusion in a scenario of a positive feedback mechanism of upper plate extension because of structure weakening through magma intrusion and subsequent decompression melting because of crustal extension (Phipps-Morgan et al. 2008).

The TSVZ and Guatemala have intermediate Sm/Lu, U/Th, and Sr/Ce, whereas CCR and the NSVZ have low U/Th and Sr/Ce and extend to the highest Sm/Lu. Although the slab beneath the TSVZ is sufficiently warm at the depth it reached beneath the arc to allow serpentine to dehydrate, the incoming plate beneath the TSVZ was possibly not serpentinised to the same degree as beneath the CSVZ. This might be due to the near-absence of fracture zones in this area (Hoernle et al. 2010). Only the Mocha Fracture Zone, not nearly as prominent a feature as the Valdivia Fracture Zone further to the south (Dzierma et al. 2012), is present outboard the TSVZ. A strong, but localised fluid signal at Volcán Nevado de Longaví, however, has been attributed to the Mocha Fracture Zone (Sellés et al. 2004; Sellés 2006), but in an arc-scale context, this is not a major fracture zone compared to those outboard the CSVZ. The fluid signal at the SSVZ is low, likely related to only incipient serpentinisation of the incoming plate, which is young and therefore warmer in this section of the arc than farther north (Völker et al. 2011).

Guatemala, CCR, and the NSVZ are characterised by shallow slabs subducting at relatively low angles and thick crust/lithosphere of the overriding plate resulting in short melting columns. Modelling results of Syracuse et al. (2010) leave ambiguity for the possibility of deserpentinisation beneath these arc segments. The estimated temperatures the slabs have reached at the respective depths beneath the arc partly coincide and partly do not coincide with the serpentine stability field, depending on the underlying model of Syracuse et al. (2010) and the

different constraints on subduction geometry by Tassara et al. (2006) (Fig. 2) versus that of Syracuse and Abers (2006) for the SVZ, and the data revision of Syracuse et al. (2010) for the CAVA compared to their earlier results. While the temperature regime might be high enough for deserpentinisation to occur beneath Guatemala, the shallow depth and corresponding lower temperature of the subducting slab beneath the volcanic front of the NSVZ and Costa Rica may limit serpentine dehydration (even if it was present in the uppermost mantle of the incoming plate). This would be consistent with a lower fluid flux and the low U/Th and Sr/Ce we observe in the arc output of the NSVZ and Costa Rica. For the more evolved melts erupted at the NSVZ, the Sr/Ce values might also have experienced a lowering through plagioclase fractionation, which is also evident from the negative Eu anomalies in Fig. 4. Although the depth of the subducting slab and the thickness of the overlying crust/lithosphere beneath Guatemala and CCR are very similar, the Sm/Lu ratios in the Costa Rica lavas extend to significantly higher values than in Guatemala. Combined with the Galapagos-type isotopic compositions of the CCR arc lavas, this is likely to reflect the contribution of melts from the incoming Galapagos hot spot track (seamount domain) (Hoernle et al. 2008) with elevated Sm/Lu. Therefore, high Sm/Lu (and other more to less incompatible element ratios of limited fluid-mobility, such as La/Yb or Nb/Y) can also reflect the presence or addition of enriched components to the mantle wedge. The higher Sm/Lu of the NSVZ as compared to the TSVZ could reflect lower degrees of melting due to a lower fluid flux, but it could also reflect the presence/addition of enriched material in the mantle wedge beneath the NSVZ. Such scenario is consistent with the enriched Sr–Nd–Hf isotopic composition of the NSVZ, since the Pb and O isotope ratios argue against assimilation of all known crustal material from this area (G. Jacques, unpublished data). Finally, the greater degree of differentiation of the NSVZ could also have contributed to the higher Sm/Lu compared to the TSVZ. Sm/Lu forms, however, no clear differentiation trend when compared to SiO_2 or Mg-number (Online Resource 4a), suggesting that magma evolution was of minor importance for the variation in Sm/Lu. In conclusion, the high ratios of more incompatible to less incompatible elements, coupled with low ratios of highly fluid-mobile to less fluid-mobile elements may either reflect lower degrees of melting due to low fluid flux beneath the volcanic front underlain by a shallow subducting slab, or be related to subducting slabs where the lower oceanic crust/upper mantle has not been substantially hydrated. Furthermore, an involvement of enriched OIB-type components, either on the subducting plate or within the mantle wedge, could generate such a combination of incompatible element ratios.

Source depletion versus source enrichment and the depth of melting

Ratios of Th, Ta, Nb, and TiO_2 to Yb are used to derive information about the composition of the source and the depth of melting (Pearce 1983, 2008). Caution must be applied when rocks that have been generated by variable degrees of melting and differentiation are compared. In these cases, the initial ratio will be shifted to higher values, because the more incompatible element (Th, Ta, Nb, and Ti) will be enriched relative to Yb, both by relatively lower degrees of melting at depth and by magma differentiation.

Plots of Th/Yb versus Nb/Yb or Ta/Yb can be used to identify depleted versus enriched mantle sources and to evaluate the role of sediment-derived supercritical fluids/melts (Pearce 1983, 2008) (Fig. 7). At all the SVZ and the CAVA, Th/Yb correlates positively with Nb/Yb, and the Th/Yb values are generally elevated compared to MORB and intra-plate basalts at a given Nb/Yb (or Ta/Yb) ratio. While the entire SVZ shows a strong arc signature, plotting in an array distant from the MORB-OIB field, a few Nicaraguan samples from small monogenetic centres at Nejapa and near Mombacho have compositions similar to E-MORB with respect to this classification.

At the SVZ, CSVZ samples display the lowest values, indicating that they are derived from the most depleted mantle sources. The TSVZ samples have intermediate and the NSVZ samples have the highest values, pointing to increasing source enrichment towards the north. No differentiation trend, however, is observable within the NSVZ sample suite when comparing these ratios with, e.g., SiO_2, Mg-number, or incompatible, fluid-immobile trace elements, and more differentiated rocks from the TSVZ do not exceed the NSVZ with regard to Th/Yb and Nb/Yb (Online Resource 4b). Samples from Nicaragua and El Salvador carry signatures of the most depleted sources amongst the CAVA rocks, while samples from Guatemala are elevated compared to an intermediately enriched mantle source and reach the most arc-like composition with the greatest enrichment of Th/Yb relative to the MORB and the intra-plate array. Rocks from Costa Rica, especially from CCR, overlap with the NSVZ. The high Costa Rican Th/Yb and Nb/Yb values (Fig. 7) reflect the derivation of OIB material through melting of the subducting Galapagos hot spot track beneath Costa Rica (Hoernle et al. 2008).

TiO_2/Yb versus Nb/Yb relationships can be instructive to constrain the depth of melting (Fig. 8) in relation to the temperature regime. In addition, a distinction can be made between enriched versus normal MORB-like source components, and possible crustal assimilation (Pearce 2008). Since TiO_2 is particularly prone to be affected by magma differentiation through fractionation of Fe–Ti-oxides, the data sets were filtered such that only samples with

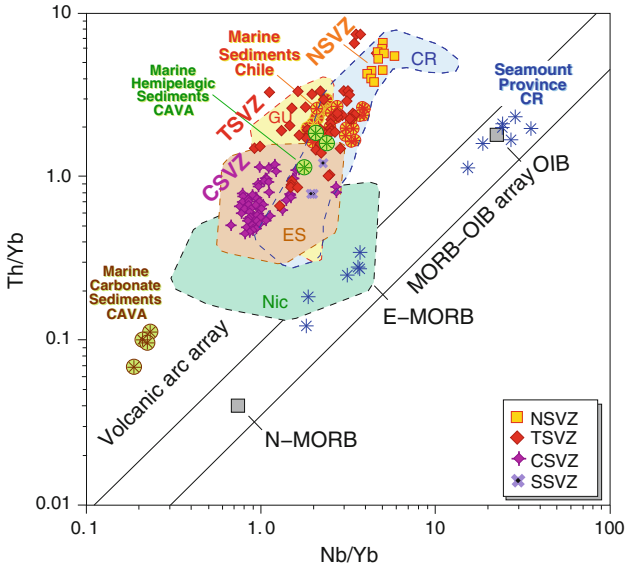

Fig. 7 Th/Yb versus Nb/Yb for the SVZ compared to the CAVA (*symbols* and *colours* as in Figs. 3 and 5), after Pearce (2008). The SVZ rocks form a positive correlation with elevated Th/Yb compared to the MORB-OIB array. Of the SVZ, the CSVZ shows the lowest Nb/Yb and Th/Yb, indicating their derivation from the most depleted mantle source, and the TSVZ has intermediate and the NSVZ has highest values, pointing to increasing source enrichment. Nicaraguan rocks partly overlap with the CSVZ, plotting in the most depleted field, including rocks with the least arc-like compositions. Compositions of input marine sediments are also shown (*asterisks*, *yellow* on *red* SVZ, Jacques et al. (2013), *red* on *yellow*: SVZ, from Lucassen et al. (2010), *green* CAVA, this study and from Heydolph et al. 2012), and they fall into the volcanic arc array. Data for the seamount province subducting beneath Costa Rica (*blue stars*) from Hoernle et al. (2000)

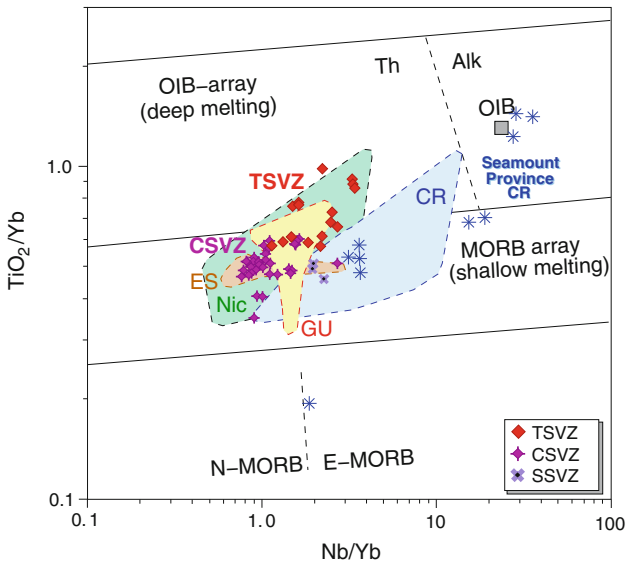

Fig. 8 TiO_2/Yb versus Nb/Yb for the SVZ compared to the CAVA (*symbols* and *colours* as in Figs. 3 and 5), after Pearce (2008). Since the TiO_2/Yb ratio is affected by oxide crystallisation, data filtering was applied: only samples for which we determined MgO $\geq$ 4 and $SiO_2 \leq$ 54.5 wt% are contained in this diagram, whereby the NSVZ becomes excluded. The TSVZ shows the deepest melting compared to the CSVZ, possibly in response to the greatest slab depth in this arc segment. At the CAVA, the Costa Rican arc segment trends towards and partly overlaps with the subducting seamount province (*blue stars*), showing the most enriched compositions. Data for the seamount province subducting beneath Costa Rica from Hoernle et al. (2000)

MgO $\geq$ 4 and $SiO_2 \leq$ 54.5 wt% are presented in Fig. 8. In the SVZ, the CSVZ samples have the most N-MORB-like composition, while the TSVZ samples have both higher Nb/Yb and TiO_2/Yb, plotting into the MORB and OIB-arrays. SSVZ samples show shallow derivation from E-MORB composition. This points to deeper melting beneath the TSVZ than in the CSVZ and SSVZ, which would be in agreement with the subduction geometry (Fig. 2a; Völker et al. 2011 after Tassara et al. 2006). CAVA rocks span a wide range in the TiO_2/Yb versus Nb/Yb diagram. The Nicaraguan and Costa Rican samples cover the entire MORB (shallow melting) array and extend into the OIB (deep melting) array. The large range and peak TiO_2/Yb ratios in the Nicaraguan samples likely respond to the great depth reached by the subducting slab and the long melting column (Fig. 2b). The high TiO_2/Yb of one Costa Rican sample from Barva volcano likely also reflects addition of melts from the seamount province of the subducting Galapagos hot spot track, of which several samples are characterised by high TiO_2/Yb.

The composition of subducted sediments and subduction fluids

Sediment subduction appears to play a key role in producing the variable compositions of the erupted materials at both arc systems. Outboard the CAVA from Nicaragua to Guatemala, the subducting sediment package consists of a ~430 m thick layer of sediments (Coulbourn et al. 1982). The lower layer (~250 m thick) consists primarily of Middle Miocene chalky carbonate ooze, whereas the upper layer (~180 m thick) consists of Middle Miocene abyssal clay and Upper Miocene to Quaternary hemipelagic diatomaceous mud (Patino et al. 2000).

With respect to Th/Yb versus Nb/Yb (Fig. 7), both the carbonate and the hemipelagic sediments plot into the volcanic arc array, and arc rocks from Nicaragua and El Salvador have compositions between the two. High Ba, Ba/La, Ba/Th, Ba/Nb, and U/Th are the characteristic for both the carbonate and the hemipelagic sediments. The carbonate sediments also have high Sr, Sr/Th, Sr/Yb, Sr/Ce, and low Nb and REE, while the hemipelagic sediments show high Cs, Th, U, Nb, and U/La (Table 1; Fig. 4d). Rocks from the volcanic front at the CAVA, in particular in Nicaragua, carry a pronounced signature of

subducted sediments (Patino et al. 2000). Since elements such as Ba and Sr are strongly enriched in particular in the marine carbonates and scavenged by subduction fluids, the erupted rocks show markedly elevated Ba and Sr concentrations compared to elements of a relatively lower fluid-mobility such as Th, Nb, and REE, resulting in high ratios of Ba/(LREE, Nb, Ta, Th), U/Th, and Sr/LREE (Figs. 5, 6a, b).

In contrast, marine sediments subducted at the Chile trench are dominated by high Pb, Cs, U, Nb, and Rb concentrations, while being comparatively depleted in Sr (Table 1; Fig. 4d). Ba is relatively depleted in the sediment samples outboard the central part of the SVZ (~36–40°S) (data from Jacques et al. 2013, Lucassen et al. 2010), whereas concentrations reach 2,250 µg/g Ba offshore the NSVZ and TSVZ (~33–36.5°S), similar to the Nicaraguan carbonate sediments (Table 1). The sediments on the incoming plate show some minor differences to those on the continental slope of the overriding plate, with the incoming plate sediments having slightly higher Ba/Th and Pb/Ce. For the interpretation of the erupted rocks with regard to their source components, a complication arises from the fact that several elements cannot be unambiguously ascribed to a unique source material (e.g. subducting sediments versus altered oceanic crust). Thorium and REE concentrations higher than in MORB are considered to be derived from subducting sediments, for they do not become enriched during hydrothermal alteration of the incoming oceanic crust. In the Th/Yb versus Nb/Yb diagram (Fig. 7), the Chilean marine sediments entirely overlap with the TSVZ. For Pb, the picture is not as straightforward, since Pb can be derived either from the basaltic layer of the downgoing plate (Plank 2005; Goss and Kay 2006) or by arc-cannibalism from Pb-rich continentally-derived volcaniclastic sediments, such as the Chilean marine sediments, or a combination of both.

In summary, the subducting sediments offshore Chile and Central America can be clearly distinguished from each other by their trace element composition, in particular with respect to Pb and Ba (Fig. 9). The arc rocks mirror the compositional differences of the sediments, with the SVZ rocks having high Pb, Pb/Ce, and Pb/Yb, while the CAVA rocks extend towards high Ba, Ba/Th, Ba/Nb, U/Th, and Sr/Ce (Figs. 5, 9). Fluids released from a dehydrating serpentinised slab have the capacity to transport the sediment signal to the arc magmas (e.g. Halama et al. 2011). Within this association, the trends formed by the arc rocks are somewhat shifted towards a Pb–Ba ratio slightly higher than that of the corresponding sediments (Fig. 9), which most likely originates from a Pb addition from the subducting ocean floor basalt. The direct compositional relationship between the subducting sediments and erupted volcanic rocks underscores the imprint of the sedimentary input into the subduction zone on the composition of the erupted arc rocks.

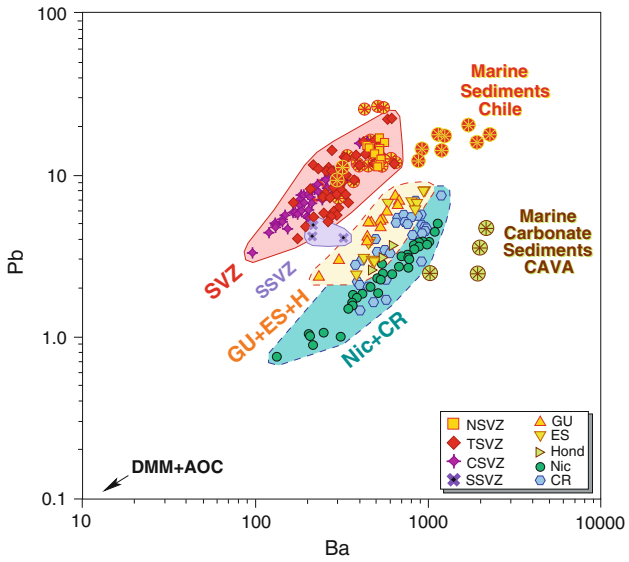

Fig. 9 Pb versus Ba for the SVZ and the CAVA, illustrating the distinct enrichment of individual fluid-mobile elements at the different arcs (*symbols* and *colours* as in Figs. 3 and 5). The SVZ is dominated by the fluid-mobile element Pb, in line with the high Pb-concentration in the marine sediments offshore southern Chile (*asterisks*, *yellow* on *red* Jacques et al. (2013), *red* on *yellow* Lucassen et al. 2010). The CAVA, in contrast, shows strongly elevated concentrations of the fluid-mobile element Ba, resulting from the Ba-enrichment of the incoming marine carbonate sediments (brown-green asterisks, this study and Heydolph et al. 2012). Data for the arrow to depleted morb mantle (DMM) and altered oceanic crust (AOC) from Salters and Stracke (2004) and Sadofsky et al. (2009), respectively

Conclusion

In this paper, we have compared two different arc systems, the continental Chilean Southern Volcanic Zone and the transitional to oceanic Central American Volcanic Arc, which display a number of different features regarding subduction geometry and geochemistry of the involved materials. The CAVA lavas, in particular those from Nicaragua, extend to very high Ba/Th, Ba/Nb, U/Th, and Sr/Ce ratios, while the Central and Southern SVZ show high Pb/Ce and Pb/U ratios. An inverse correlation exists between highly fluid-mobile to less fluid-mobile element ratios and proxies for degree of melting (e.g. Sm/Lu) whereby the CSVZ in Chile is most similar to the oceanic-like Nicaragua/El Salvador at the CAVA, showing the highest degrees of melting and/or derivation from the most depleted mantle sources. Costa Rica and the NSVZ have the highest Sm/Lu and La/Yb, which most likely reflects a combination of low degrees of melting and derivation from

enriched mantle sources, as well as differentiation for the more evolved NSVZ lavas.

The type of fluid signal is fundamentally different between the SVZ and the CAVA such that arc rocks at the SVZ show high Pb, while the CAVA is characterised by strongly elevated Ba. The same compositional difference is displayed by the subducting marine sediments with high Pb offshore the SVZ, and high Ba outboard the CAVA, pointing to a clear compositional relationship between the subducted sediments and the subduction fluids/hydrous melts they release. This geochemical signal is preserved during infiltration of the fluids into the mantle wedge and formation of arc magmas, and likely recycled back into the system by deposition of arc volcanic ejecta onto the ocean floor. In conclusion, the sedimentary input into the subduction system appears to have the greatest effect on the composition of fluid-mobile elements in the arc rocks, with high concentrations in the sediments and ratios of highly fluid-mobile to less fluid-mobile elements (e.g. Ba/Th, Ba/Nb, U/Th, Sr/Ce, Pb/Ce, and Pb/U), whereas the composition of the mantle wedge (enriched versus depleted) and the depth and degrees of melting appear to control the variations in the ratios highly incompatible to less incompatible, relatively immobile elements (e.g. Nb/Yb, Ta/Yb, La/Yb, Sm/Lu, and Nb/Y).

Acknowledgments We sincerely thank Julian Pearce and an anonymous reviewer for constructive comments that improved the manuscript. Ralf Halama is acknowledged for comments and for the editorial handling of the paper. We would also like to thank Paul van den Bogaard, Luis Lara, Jorge Clavero, Daniel Sellés, Katja Hockun, and Rayén Rivera-Vidal for their assistance in the field. The Chilean arrieros Titin, Gerardo, Valdemar, Roberto, Nano, and their colleagues are acknowledged for providing horses and guidance in difficult terrains on Chilean volcanoes. We are grateful to Eduardo Boisset for his excellent performance during helicopter-based sampling campaigns in the high Andes. David Völker and the crew of the RV Sonne cruise 210 are thanked for obtaining and providing the marine sediment samples offshore Chile. Ken Heydolph contributed fruitful comments and discussion. Credit is due to Philipp Rohde and Silvia Gütschow for their assistance with the sample preparation and to Ulrike Westernströer for her help with the ICP-MS analyses. This paper is contribution No. 254 of Sonderforschungsbereich 574 "Volatiles and Fluids in Subduction Zones", funded by the German Research Foundation.

References

Abers GA, van Keken PE, Kneller EA, Ferris A, Stachnik JC (2006) The thermal structure of subduction zones constrained by seismic imaging: implications for slab dehydration and wedge flow. Earth Planet Sci Lett 241(3–4):387–397. doi:10.1016/j.epsl.2005.11.055

Aubouin J, von Huene R (1982) Initial reports of the Deep Sea Drilling Project, vol 67. Washington DC, U.S. Government Printing Office, 799 p

Bangs NL, Cande SC (1997) Episodic development of a convergent margin inferred from structures and processes along the southern Chile margin. Tectonics 16(3):489–503

Benjamin ER, Plank T, Wade JA, Kelley KA, Hauri EH, Alvarado GE (2007) High water contents in basaltic magmas from Irazú Volcano, Costa Rica. J Volcanol Geotherm Res 168:68–92. doi:10.1016/j.jvolgeores.2007.08.008

Carr MJ (1984) Symmetrical and segmented variation of physical and geochemical characteristics of the Central American volcanic front. J Volcanol Geotherm Res 20:231–252

Carr MJ, Feigenson MD, Bennett EA (1990) Incompatible element and isotopic evidence for tectonic control of source mixing and melt extraction along the Central American Volcanic Arc. Contrib Mineral Petrol 105:369–380. doi:10.1007/BF00286825

Carr MJ, Saginor I, Alvarado GE, Bolge LL, Lindsay FN, Milidakis K, Turrin BD, Feigenson MD, Swisher CC III (2007) Element fluxes from the volcanic front of Nicaragua and Costa Rica. Geochem Geophys Geosyst 8:Q06001. doi:10.1029/2006GC001396

Cooper LB, Ruscitto DM, Plank T, Wallace PJ, Syracuse EM, Manning CE (2012) Global variations in H_2O/Ce: 1. Slab surface temperatures beneath volcanic arcs. Geochem Geophys Geosyst 13:Q03024. doi:10.1029/2011GC003902

Coulbourn WT, Hesse R, Azema J, Shiki T (1982) A summary of the sedimentology of DSDP leg 67 sites: the Middle America trench and slope of Guatemala—an active margin transect. In: Aubouin J et al (eds) Initial reports DSDP 67:759–774

Davidson JP, Dungan MA, Ferguson KM, Colucci MT (1987) Crust-magma interactions and the evolution of arc magmas: the San Pedro-Pellado volcanic complex, southern Chilean Andes. Geology 15:443–446

DeMets C (2001) A new estimate for present-day Cocos-Caribbean plate motion: implications for slip along the Central American Volcanic Arc. Geophys Res Let 28:4043–4046

Dungan MA, Wulff A, Thomson R (2001) Eruptive stratigraphy of the Tatara-San Pedro complex, 36°S, Southern Volcanic Zone, Chilean Andes: reconstruction method and implications for magma evolution at long-lived arc volcanic centers. J Petrol 42(3):555–626

Dzierma Y, Rabbel W, Thorwart M, Koulakov I, Wehrmann H, Hoernle K, Comte D (2012) Seismic velocity structure of the slab and continental plate in the region of the 1960 Valdivia (Chile) slip maximum—insights into fluid release and plate coupling. Earth Planet Sci Lett 331/332C:164–176. doi:10.1016/j.epsl.2012.02.006

Eiler JM, Carr MJ, Reagan M, Stolper E (2005) Oxygen isotope constraints on the sources of Central American arc lavas. Geochem Geophys Geosyst 6:Q07007. doi:10.1029/2004GC000804

Ferguson KM, Dungan MA, Davidson JP, Colucci MT (1992) The Tatara-San Pedro Volcano, 36 °S Chile: a chemically variable, dominantly mafic magmatic system. J Petrol 33(1):1–43

Garbe-Schönberg CD (1993) Simultaneous determination of thirty-seven trace elements in twenty-eight international rock standards by ICP-MS. Geostand Newsl 17:81–97. doi:10.1111/j.1751-908X.1993.tb00122.x

Gazel E, Carr MJ, Hoernle K, Feigenson MD, Szymanski D, Hauff F, van den Bogaard P (2009) Galapagos-OIB signature in southern Central America: mantle refertilization by arc—hot spot interaction. Geochem Geophys Geosyst 10:Q02S11. doi:10.1029/2008GC002246

Geldmacher J, Hoernle K, van den Bogaard P, Hauff F, Klügel A (2008) Age and geochemistry of the Central American forearc basement (DSDP Leg 67 and 84): insights into Mesozoic arc volcanism and seamount accretion on the fringe of the Caribbean LIP. J Petrol 49(10):1781–1815. doi:10.1093/petrology/egn046

Geldmacher J, Höfig T, Hauff F, Hoernle K, Garbe-Schönberg D, Wilson DS (2013) Influence of the Galápagos hotspot on the East Pacific Rise during Miocene superfast spreading. Geology 41:183–186. doi:10.1130/G33533.1

Goss A, Kay SM (2006) Steep REE patterns and enriched Pb isotopes in southern Central American arc magmas: evidence for forearc subduction erosion? Geochem Geophys Geosyst 7:Q05016. doi:10.1029/2005GC001163

Grevemeyer I, Ranero CR, Flueh ER, Kläschen D, Bialas J (2007) Passive and active seismological study of bending-related faulting and mantle serpentinization at the Middle America trench. Earth Planet Sci Lett 258:528–542. doi:10.1016/j.epsl.2007.04.013

Grove TL, Baker MB (1984) Phase equilibrium controls on the tholeiitic versus calc-alkaline differentiation trends. J Geophys Res 89/B5:3253–3274

Hacker BR (2008) H2O subduction beyond arcs. Geochem Geophys Geosyst 9(3):Q03001. doi:10.1029/2007GC001707

Halama R, John T, Herms P, Hauff F, Schenk V (2011) A stable (Li, O) and radiogenic (Sr, Nd) isotope perspective on metasomatic processes in a subducting slab. Chem Geol 281:151–166. doi:10.1016/j.chemgeo.2010.12.001

Heydolph K, Hoernle K, Hauff F, van den Bogaard P, Portnyagin M, Bindeman I, Garbe-Schönberg D (2012) Along and across arc geochemical variations in NW Central America: evidence for involvement of lithospheric pyroxenite. Geochim Cosmochim Acta 84:459–491. doi:10.1016/j.gca.2012.01.035

Hickey RL, Gerlach DC, Frey FA (1984) Geochemical variations in volcanic rocks from central-south Chile (33°–42°S). In: Harmon RS, Barreiro BA (eds) Andean Magmatism: chemical and isotopic constraints. Shiva Publishing, Cheshire, England, pp 72–95

Hildreth W, Moorbath S (1988) Crustal contributions to arc magmatism in the Andes. Contrib Mineral Petrol 98:455–489

Hoernle K, Werner R, Phipps-Morgan J, Garbe-Schönberg D, Bryce J, Mrazek J (2000) Existence of complex spatial zoning in the Galapagos Plume. Geology 28:435–438. doi:10.1130/0091-7613(2000)28<435:EOCSZI>2.0.CO;2

Hoernle K, Tilton G, le Bas MJ, Duggen S, Garbe-Schönberg D (2002) Geochemistry of oceanic carbonatites compared with continental carbonatites: mantle recycling of oceanic crustal carbonate. Contrib Mineral Petrol 142:520–542. doi:10.1007/s004100100308

Hoernle K, Abt DL, Fischer KM, Nichols H, Hauff F, Abers G, van den Bogaard P, Alvarado G, Protti JM, Strauch W (2008) Geochemical and geophysical evidence for arc-parallel flow in the mantle wedge beneath Costa Rica and Nicaragua. Nature 451:1094–1097. doi:10.1038/nature06550

Hoernle K, Hauff F, Hanan F, Werner R, Christie D, Garbe-Schönberg D (2010) Seamount South of the Galapagos Spreading Center provide new constraints on plume-ridge interaction and evidence for a depleted plume component. Eos Trans AGU 91(52), Fall Meet Suppl, Abstract V52A-08

Hofman AV, Jochum KP, Seufert M, White WM (1986) Nb and Pb in oceanic basalts: new constraints on mantle evolution. Earth Planet Sci Lett 79:33–45

Ivandic M, Grevemeyer I, Berhorst A, Flueh ER, McIntosh K (2007) Impact of bending related faulting on the seismic properties of the incoming oceanic plate offshore of Nicaragua. J Geophys Res 113:B05410. doi:10.1029/2007JB005291

Jacques G, Hoernle K, Gill J, Hauff F, Wehrmann H, Garbe-Schönberg D, van den Bogaard P, Bindeman I, Lara LE (2013) Across-arc geochemical variations in the Southern Volcanic Zone, Chile (34.5–38.0°S): constraints on mantle wedge and input compositions. Geochim Cosmochim Acta. doi:10.1016/j.gca.2013.05.016

Jicha BR, Smith KE, Singer BS, Beard BL, Johnson CM, Rogers NW (2010) Crustal assimilation no match for slab fluids beneath Volcán de Santa María, Guatemala. Geology 38:859–862. doi:10.1130/G31062.1

John T, Scambelluri M, Frische M, Barnes JD, Bach W (2011) Dehydration of subducting serpentinite: implications for halogen mobility in subduction zones and the deep halogen cycle. Earth Planet Sci Lett 308:65–76. doi:10.1016/j.epsl.2011.05.038

Kay RW, Kay SM (1993) Delamination and delamination magmatism. Tectonophysics 219:177–189

Kay SM, Mpodozis C (2002) Magmatism as a probe to the Neogene shallowing of the Nazca plate beneath the modern Chilean flat-slab. J South Am Earth Sci 15:39–57

Kessel R, Schmidt MW, Ulmer P, Pettke T (2005) Trace element signature of subduction-zone fluids, melts and supercritical liquids at 120–180 km depth. Nature 437:724–727. doi:10.1038/nature03971

LeMaitre RW, Bateman P, Dudek A, Keller J, Lameyre J, Le Bas MJ, Sabine PA, Schmid R, Sorensen H, Streckeisen A, Woolley RA, Zanettin B (1989) A classification of igneous rocks and glossary of terms, recommendations of the International Union of Geological Sciences Subcommission on the systematics of igneous rocks, vol 193. Blackwell Scientific, Oxford

López-Escobar L, Parada MA, Moreno H, Frey FA, Hickey-Vargas R (1992) A contribution to the petrogenesis of Osorno and Calbuco volcanoes, Southern Andes (41°00′–41°30′S): comparative study. Rev Geol Chile 19:211–226

Lucassen F, Wiedecke M, Franz G (2010) Complete recycling of a magmatic arc: evidence from chemical and isotopic composition of Quaternary trench sediments in Chile (36°–40°S). Int J Earth Sci 99:687–701. doi:10.1007/s00531-008-0410-4

MacKenzie L, Abers GA, Fisher KM, Syracuse EM, Protti JM, Gonzales V, Strauch W (2008) Crustal structure along the southern Central American volcanic front. Geochem Geophys Geosyst 9/8:Q08S09. doi:10.1029/2008GC001991

Melnick D, Echtler HP (2006) Inversion of forearc basins in south-central Chile caused by rapid glacial age trench fill. Geology 34(9):709–712. doi:10.1130/G22440.1

Patino LC, Carr MJ, Feigenson MD (2000) Local and regional variations in Central American arc lavas controlled by variations in subducted sediment input. Contrib Mineral Petrol 138(3):265–283

Peacock SM, van Keken PE, Holloway SD, Hacker BR, Abers GA, Fergason RL (2005) Thermal structure of the Costa Rica—Nicaragua subduction zone. Phys Earth Planet Int 149:187–200. doi:10.1016/j.pepi.2004.08.030

Pearce JA (1983) Role of the sub-continental lithosphere in magma genesis at active continental margins. In: Hawkesworth C, Norry M (eds) Continental basalts and mantle xenoliths. Shiva Geology Series, Nantwich, pp 230–249

Pearce JA (2008) Geochemical fingerprinting of oceanic basalts with applications to ophiolite classification and the search for Archean oceanic crust. Lithos 100:14–48. doi:10.1016/j.lithos.2007.06.016

Phipps-Morgan J, Ranero C, Vanucchi P (2008) Intra-arc extension in Central America: links between plate motions, tectonics, volcanism, and geochemistry. Earth Planet Sci Lett 272:365–371. doi:10.1016/j.epsl.2008.05.004

Plank T (2005) Constraints from Thorium/Lanthanum on sediment recycling at subduction zones and the evolution of the continents. J Petrol 46(5):921–944. doi:10.1093/petrology/egi005

Plank T, Langmuir CH (1993) Tracing trace elements from sediment input to volcanic output at subduction zones. Nature 362:739–743

Plank T, Balzer V, Carr M (2002) Nicaraguan Volcanoes record paleoceanographic changes accompanying closure of the Panama gateway. Geology 30(12):1087–1090. doi:10.1130/0091-7613(2002)030

Ranero C, Phipps Morgan J, McIntosh K, Reichert C (2003) Bending-related faulting and mantle serpentinization at the Middle America trench. Nature 425:367–373. doi:10.1038/nature01961

Reagan M, Gill J (1989) Coexisting calcalkaline and high-niobium basalts from Turrialba volcano, Costa Rica: implications for residual titanates in arc magma sources. J Geophys Res 94:4619–4633. doi:10.1029/JB094iB04p04619

Reubi O, Bourdon B, Dungan MA, Koornneef JM, Sellés D, Langmuir CH, Aciego S (2011) Assimilation of the plutonic roots of the Andean arc controls variations in U-series disequilibria at Volcán Llaima, Chile. Earth Planet Sci Lett 303:37–47. doi:10.1016/j.epsl.2010.12.018

Rickwood PC (1989) Boundary lines within petrologic diagrams which use oxides of major and minor elements. Lithos 22:247–263

Rychert CA, Fischer KM, Abers GA, Plank T, Syracuse E, Protti JM, Gonzales V, Strauch W (2008) Strong along-arc variations in attenuation in the mantle wedge beneath Costa Rica and Nicaragua. Gechem Geophys Geosyst 9:Q10S10. doi:10.1029/2008GC002040

Sadofsky SJ, Portnyagin MV, Hoernle K, van den Bogaard P (2008) Subduction cycling of volatile and trace elements through the Central American volcanic arc: evidence from melt inclusions. Contrib Mineral Petrol 155(4):433–456. doi:10.1007/s00410-007-0251-3

Sadofsky SJ, Hoernle K, Duggen S, Hauff F, Werner R (2009) Geochemical variations on the Cocos Plate subducting offshore of Central America. Int J Earth Sci 98:901–913. doi:10.1007/s00531-007-0289-5

Salters VJM, Stracke A (2004) Composition of the depleted mantle. Geochem Geophys Geosyst 5(5):Q05004. doi:10.1029/2003GC000597

Savov IP, Ryan JG, D'Antonio M, Fryer P (2007) Shallow slab fluid release across and along the Mariana arc-basin system: insights from geochemistry of serpentinized peridotites from the Mariana fore arc. J Geophys Res 112:B09205. doi:10.1029/2006JB004749

Sellés D (2006) Stratigraphy, petrology, and geochemistry of Nevado de Longaví volcano, Chilean Andes (36.2°S). PhD thesis, Université de Geneve, 103 p

Sellés D, Rodríguez C, Dungan MA, Naranjo J, Gardeweg M (2004) Geochemistry of Nevado de Longaví volcano (36.2°S): a compositionally atypical arc volcano in the Southern Volcanic Zone of the Andes. Rev Geol Chile 31:293–315

Sisson TW, Grove TL (1993) Experimental investigations of the role of H_2O in calc-alkaline differentiation and subduction zone magmatism. Contrib Mineral Petrol 113:143–166

Spandler C, Hermann J, Faure K, Mavrogenes JA, Arculus RJ (2008) The importance of talc and chlorite ''hybrid'' rocks for volatile recycling through subduction zones; evidence from the high-pressure subduction melange of New Caledonia. Contrib Mineral Petrol 155:181–198. doi:10.1007/s00410-007-0236-2

Stern CR (2004) Active Andean volcanism: its geologic and tectonic setting. Rev Geol Chile 31(2):161–206

Sun SS, McDonough WF (1989) Chemical and isotopic systematics of oceanic basalts: implications for mantle composition and processes. Geol Soc London Spec Pub 42:313–345. doi:10.1144/GSL.SP.1989.042.01.19

Syracuse EM, Abers GA (2006) Global compilation of variations in slab depth beneath arc volcanoes and implications. Geochem Geophys Geosys 7(5):Q05017. doi:10.1029/2005GC001045

Syracuse EM, van Keken PE, Abers GA (2010) The global range of subduction zone thermal models. Phys Earth Planet Interiors 183:73–90. doi:10.1016/j.pepi.2010.02.004

Tassara A, Götze HJ, Schmidt S, Hackney R (2006) Three-dimensional density model of the Nazca plate and the Andean continental margin. J Geophys Res 111(B09404). doi:10.1029/2005JB003976

Tatsumi Y (1986) Formation of the volcanic front in subduction zones. Geophys Res Let 13(8):717–720

Tera F, Brown L, Morris J, Sacks IS, Klein J, Middleton R (1986) Sediment incorporation in island-arc magmas: inferences from ^{10}Be. Geochim Cosmochim Acta 50:535–550. doi:10.1016/016-7037(86)90103-1

Ulmer P, Trommsdorff V (1999) Phase relations of hydrous mantle subducting to 300 km. In: Fei Y, Bertka N, Mysen BO (eds) Mantle petrology: field observations and high pressure experimentation. Geochemical Society of Special Publication 6:259–281

van Keken PE, Hacker BR, Syracuse EM, Abers GA (2011) Subduction factory: 4. Depth-dependent flux of H_2O from subducting slabs worldwide. J Geophys Res 116(B01401). doi:10.1029/2010JB007922

Völker D, Kutterolf S, Wehrmann H (2011) Comparative mass balance of volcanic edifices at the Southern Volcanic Zone of the Andes between 33°S and 46°S. J Volc Geotherm Res 205:114–129. doi:10.1016/j.volgeores.2011.03.011

von Huene R, Scholl DW (1991) Observations concerning sediment subduction and subduction erosion, and the growth of continental crust at convergent ocean margins. Rev Geophys 29:279–316

Watt SFL, Pyle DM, Mather TA (2011) Geology, petrology and geochemistry of the dome complex of Huequi volcano, southern Chile. Andean Geol 38(1):335–348

Wehrmann H, Hoernle K, Jacques G, Garbe-Schönberg D, Schumann K, Mahlke J, Lara L (in review/this volume) Volatile (sulphur and chlorine), major, and trace element geochemistry of mafic to intermediate tephras from the Chilean Southern Volcanic Zone (33–43°S). Int J Earth Sci

Wehrmann H, Hoernle K, Portnyagin M, Wiedenbeck M, Heydolph K (2011) Volcanic CO_2 output at the Central American subduction zone inferred from melt inclusions in olivine crystals from mafic tephras. Geochem Geophys Geosys 12(6):Q06003. doi:10.1029/2010GC003412

Werner R, Hoernle K, van den Bogaard P, Ranero C, von Huene R, Korich D (1999) Drowned 14-m.y.-old Galapagos Archipelago off the coast of Costa Rica; implications for tectonic and evolutionary models. Geology 27:499–502. doi:10.1130/0091-7613(1999)027<0499:DMYOGP>2.3.CO;2

Werner R, Hoernle K, Barckhausen U, Hauff F (2003) Geodynamic evolution of the Galápagos hot spot system (central east Pacific) over the past 20 m.y.: constraints from morphology, geochemistry, and magnetic anomalies. Geochem Geophys Geosyst 4(12):1108. doi:10.1029/2003GC000576